Available online at www.sciencedirect.com
ScienceDirect
Journal of the European Ceramic Society 31 (2011) 1915–1920
www.elsevier.com/locate/jeurceramsoc

Effect of TiO_2 addition on grain shape and grain coarsening behavior in $95Na_{1/2}Bi_{1/2}TiO_3$–$5BaTiO_3$

Kyoung-Seok Moon [a,1], Dibyaranjan Rout [a], Ho-Yong Lee [b], Suk-Joong L. Kang [a,*]

[a] *Department of Materials Science and Engineering, Korea Advanced Institute of Science and Technology, 335 Gwahak-ro, Yuseong-gu, Daejeon 305-701, Republic of Korea*

[b] *Department of Materials Science and Engineering, Sun Moon University, Asan 336-708, Republic of Korea*

Received 22 October 2010; received in revised form 23 March 2011; accepted 3 April 2011
Available online 6 May 2011

Abstract

Grain coarsening behavior in the $95Na_{1/2}Bi_{1/2}TiO_3$–$5BaTiO_3$ system has been studied as a function of the addition of TiO_2. As the amount of added TiO_2 was increased, the grain shape changed to a more faceted cube, indicating an increase in the step free energy of the facets, and hence a rise in the critical driving force for appreciable growth of grains. Grain coarsening behavior also changed from pseudo-normal to abnormal with an increasing TiO_2 concentration and thus increased faceting. The pseudo-normal behavior observed in the system without TiO_2 addition also changed to quite abnormal behavior during extended sintering. These observations support our theoretical prediction based on the coupling effects between the maximum driving force for growth and the critical driving force for appreciable growth.

Keyword: Grain growth; Interface; Perovskite; Microstructure-final; Lead-free piezoelectric

1. Introduction

Many investigations[1–20] have shown a close relationship between the coarsening behavior of grains in polycrystals and the equilibrium shape of grains. Abnormal grain coarsening (AGC) is frequently observed in faceted systems with smooth (atomically ordered) interfaces[4–20] whereas normal grain coarsening (NGC) occurs in systems with rough (atomically disordered) interfaces.[1–3] The NGC observed in systems with rounded grains has been attributed to diffusion-controlled growth due to an unlimited number of nucleation sites for atom attachment at the rough interface.[15,16,20] The coarsening kinetics governed by diffusion obeys the cubic law according to the classical theory developed by Lifshitz and Slyozov,[21] and Wagner.[22] In contrast, the growth of faceted grains with atomically ordered interfaces is governed either by interface reaction or by diffusion (mixed control) for driving forces for growth below or above a critical value (Δg_c), respectively, as schematically shown in Fig. 1. As a result, non-normal grain coarsening occurs.[15,19,20]

Our recent calculation predicted that the type of grain coarsening, including nonstationary and stationary in terms of the variation of relative grain size distribution with annealing time, is governed by the relative value between the maximum driving force for growth, Δg_{max}, and the critical driving force for appreciable growth, Δg_c.[19] The maximum driving force is governed by the grain size and distribution while the critical driving force is controlled by the step free energy and temperature.[19,20] Therefore, for a given Δg_{max}, the grain coarsening behavior is predicted to change with the step free energy: stagnant grain coarsening (SGC) for $\Delta g_c \gg \Delta g_{max}$, abnormal grain coarsening for $\Delta g_c \leq \Delta g_{max}$, pseudo-normal grain coarsening (PNGC) for $0 < \Delta g_c \ll \Delta g_{max}$, and normal grain coarsening for $\Delta g_c = 0$.

* Corresponding author. Tel.: +82 42 350 4113; fax: +82 42 350 8920.
E-mail address: sjkang@kaist.ac.kr (S.-J.L. Kang).
[1] Current address: Advanced Materials Research Center, Samsung Advanced Institute of Technology, Giheung-gu, Yongin-si, Gyeonggi-do 446-712, Republic of Korea.

0955-2219/$ – see front matter © 2011 Elsevier Ltd. All rights reserved.
doi:10.1016/j.jeurceramsoc.2011.04.002

Fig. 1. Schematic representation showing the growth rate of a crystal as a function of the driving force for diffusion (dashed line) and mixed (diffusion and interface reaction) control (solid lines) mechanisms. For mixed control, three curves are plotted for undoped (0T), 0.7 mol% TiO_2-doped (0.7T), and 1.5 mol% TiO_2-doped $95Na_{1/2}Bi_{1/2}TiO_3$–$5BaTiO_3$ (1.5T) samples. The dotted curve is a schematic plot of grain size distribution with respect to the driving force for the 1.5T sample.

The grain coarsening behavior in a system with non-zero Δg_c, however, can vary with the annealing time (nonstationary grain coarsening) due to the change (in most cases, reduction) in Δg_{max} during annealing.[19,20,23]

With respect to the relative value between Δg_{max} and Δg_c, the variation of the grain size distribution with annealing time is the key factor to identify the coarsening behavior. NGC is characterized by a unimodal size distribution with annealing time while AGC is described by a bimodal distribution with some (or a few) abnormally large grains embedded in a fine matrix. PNGC can be defined as coarsening behavior between NGC and AGC. It is characterized by a variable size distribution with annealing time while maintaining a unimodal distribution.[19,20,23] On the other hand, SGC exhibits essentially no grain coarsening during the time period of observation.

Some experimental studies have shown that the grain coarsening behavior was abnormal and normal for faceted and rounded grains, respectively, in the same system by changing temperature,[14,24] adding dopants,[7,8,11,17,25] or varying oxygen partial pressure.[8,26,27] Cho et al.[14] studied the effect of temperature on grain shape and grain coarsening behavior in the NbC–Co system. They observed a change in grain shape from faceted to rounded and also a change in coarsening behavior from abnormal to (pseudo-)normal with increasing sintering temperature. Choi et al.[10] studied the effect of Ti substitution in NbC on the grain shape and grain coarsening behavior in the $Nb_{1-x}Ti_xC$–Co system. With Ti substitution, the grain shape changed from round-edged cube to well-faceted cube and abnormal coarsening behavior became more distinctive. Chung et al.[8] studied the effects of oxygen partial pressure and donor doping on the grain shape and grain coarsening behavior in Ti-excess $SrTiO_3$. When the estimated total vacancy concentration was high or low, the grain shape was rounded or faceted, and normal or abnormal coarsening occurred, respectively. These previous studies demonstrate the correlation between grain shape and grain coarsening behaviors: normal for rounded grains and abnormal for faceted grains in the same system. They, however, did not show a detailed change in grain coarsening behavior with sintering time for various shapes of grains.

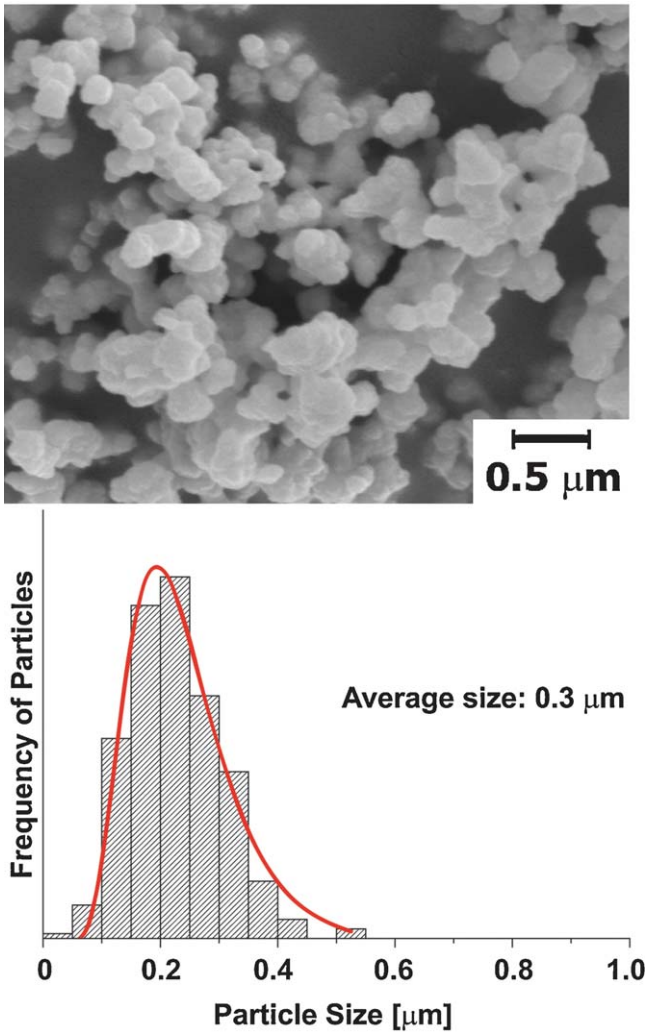

Fig. 2. SEM micrograph of synthesized NBT–5BT powder and its size distribution.

The purpose of this study is to provide experimental support for the predicted effect of the change in step free energy, i.e. grain shape, on grain coarsening behavior in a partially faceted system, $95Na_{1/2}Bi_{1/2}TiO_3$–$5BaTiO_3$ (NBT–5BT). This system is also of technological importance as a lead-free piezoelectric material. The grain shape (step free energy) was systematically varied with the addition of varying amounts of TiO_2.

2. Experimental procedure

Polycrystalline $95Na_{1/2}Bi_{1/2}TiO_3$–$5BaTiO_3$ ceramic samples were prepared from commercial powders of Na_2CO_3 (Acros Organics, NJ, USA), Bi_2O_3 (Kojundo Chemical Lab Co., Saitama, Japan), $BaCO_3$ (Sigma–Aldrich, St. Louis, USA) and TiO_2 (Sigma–Aldrich, St. Louis, USA). The proportioned powders were ball-milled for 24 h in ethanol using a polypropylene jar and 5 mm sized ZrO_2 balls. The dried slurry was crushed and passed through a 150 mesh sieve. The powders were calcined in

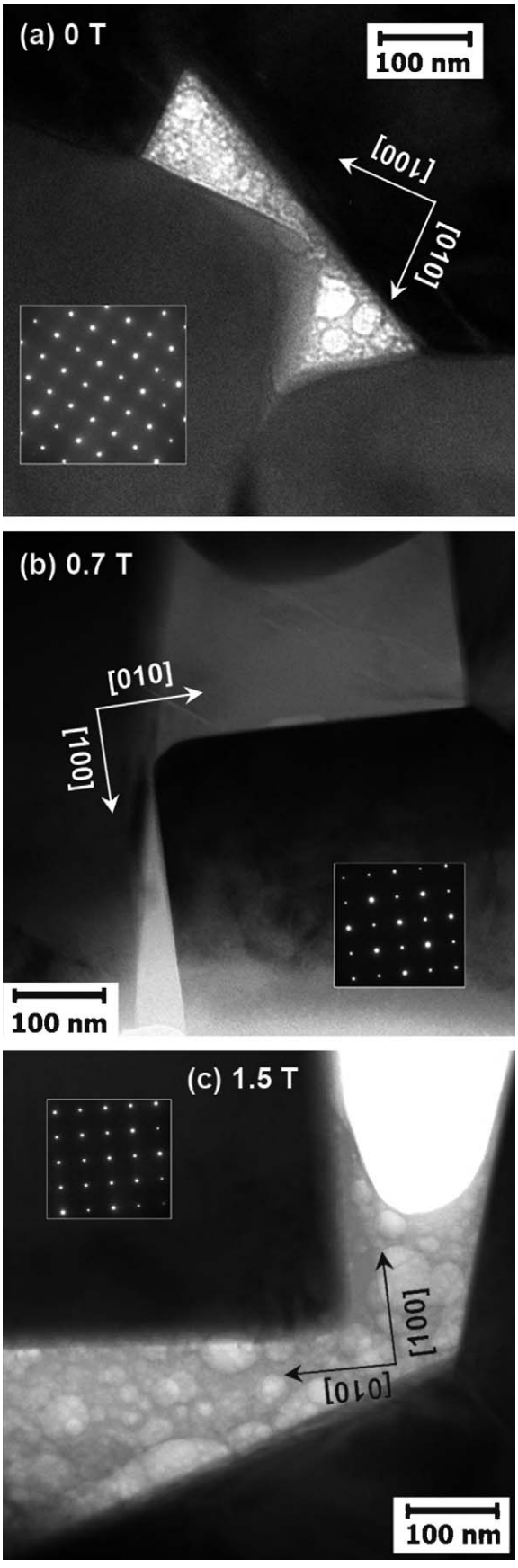

Fig. 3. TEM micrographs and their selected area diffraction patterns along [1 0 0] of (a) undoped (0T), (b) 0.7 mol% (0.7T), and (c) 1.5 mol% TiO_2-doped $0.95Na_{1/2}Bi_{1/2}TiO_3$–$0.05BaTiO_3$ (1.5T) sintered at 1200 °C for 1 h.

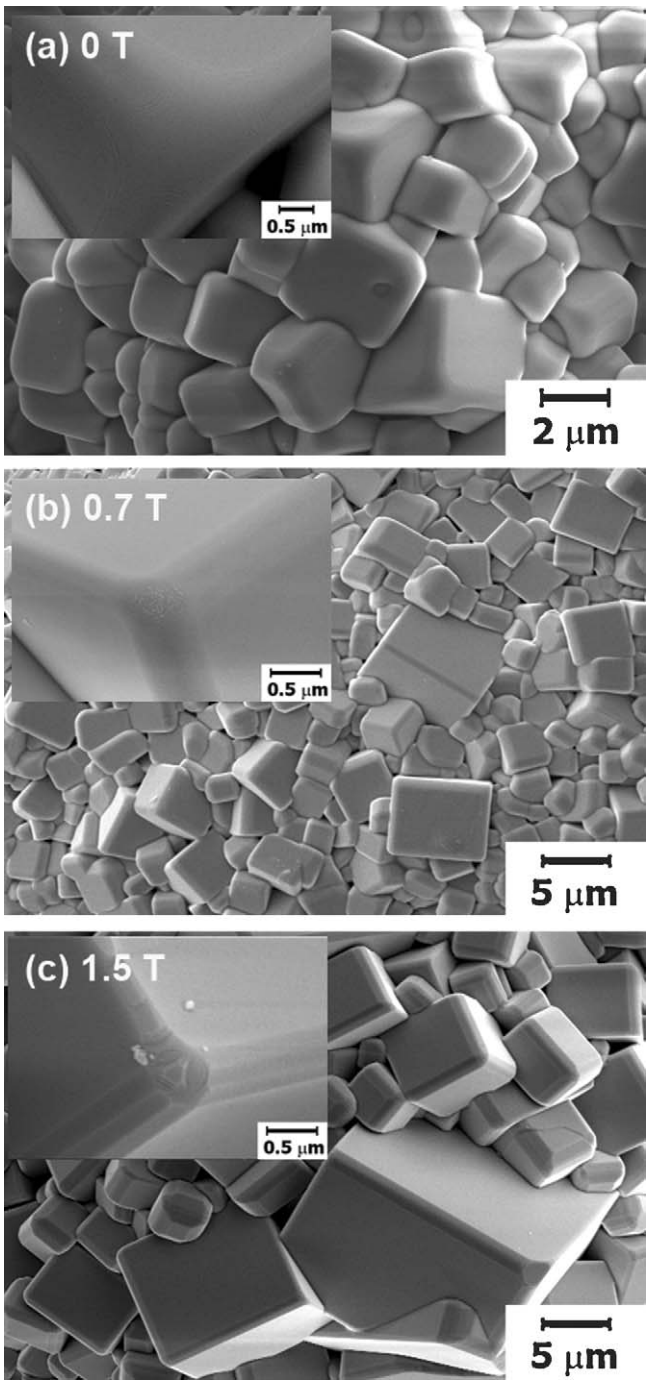

Fig. 4. SEM micrographs of (a) undoped (0T),[23] (b) 0.7 mol% (0.7T), and (c) 1.5 mol% TiO_2-doped $0.95Na_{1/2}Bi_{1/2}TiO_3$–$0.05BaTiO_3$ (1.5T) powders annealed at 1200 °C for 10 h.

an alumina crucible at 800 °C for 4 h in air. The calcined powder without or with TiO_2 addition of 0.7 and 1.5 mol% TiO_2 (denoted as 0.7T and 1.5T) was separately ball-milled for 24 h. After ball milling, the slurry was again dried and crushed in a mortar using a pestle. Fig. 2 shows the shape of the prepared NBT–5BT powder and its size distribution measured by an image analysis (more details follow in the next paragraph). The distribution with an average size of 0.3 μm is quite narrow and fits a lognormal curve (a thin red line).

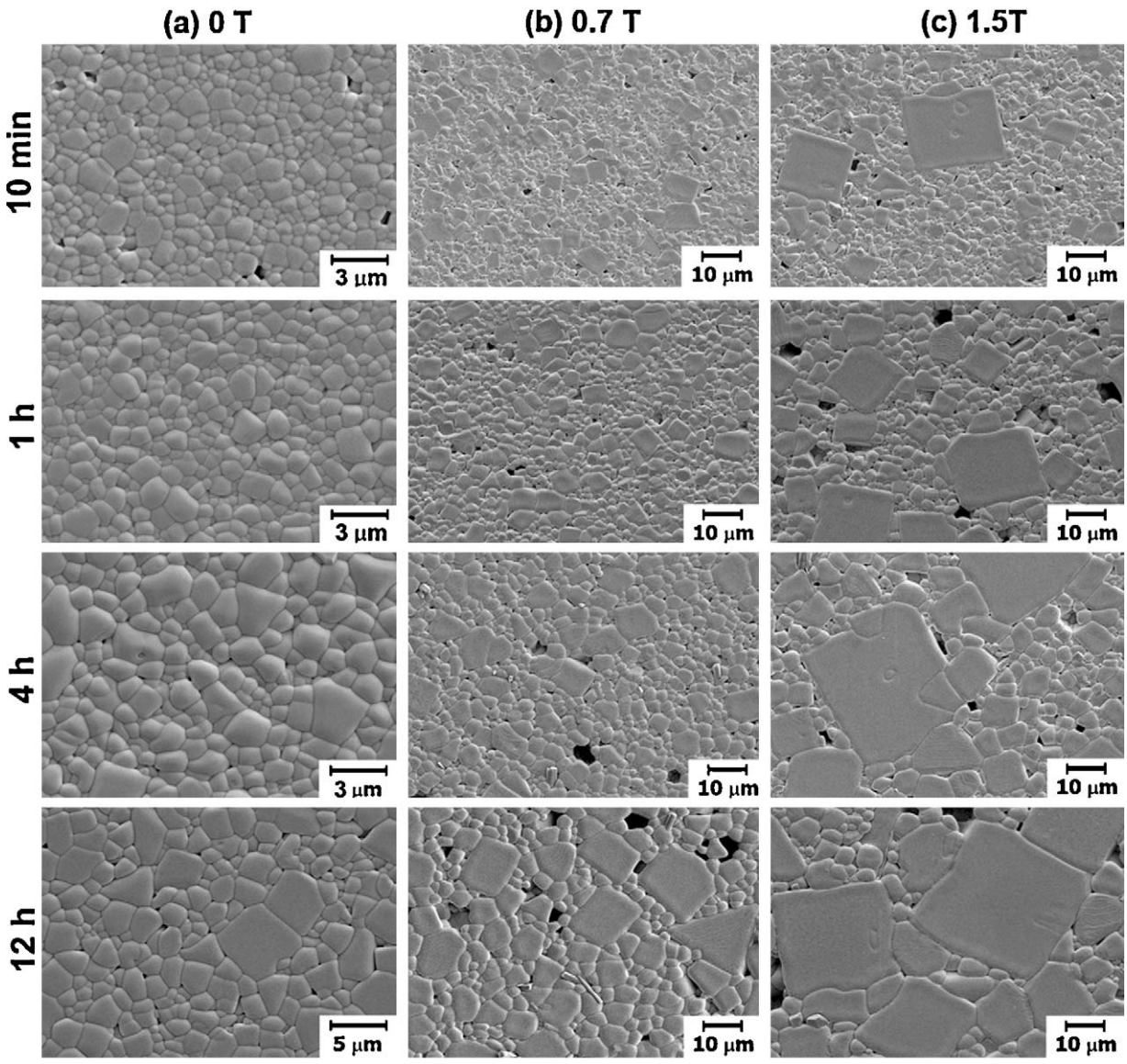

Fig. 5. SEM micrographs of (a) undoped (0T),[23] (b) 0.7 mol% (0.7T), and (b) 1.5 mol% TiO_2-doped $0.95Na_{1/2}Bi_{1/2}TiO_3$–$0.05BaTiO_3$ (1.5T) sintered at 1200 °C for various times.

Powder compacts of 14 mm diameter and ~4 mm thickness were prepared by hand pressing in a stainless steel die and then cold isostatically pressed at 200 MPa. The compacts were then sintered at 1200 °C for different duration of time intervals (10 min, 1 h, 4 h, and 12 h) on a Pt plate in an alumina crucible with a lid in air. The heating and cooling rates were 4 °C/min. The grain shape was observed under a scanning electron microscope (SEM) as well as a transmission electron microscope (TEM). The SEM samples were prepared by sintering NBT–5BT powder samples with and without TiO_2 doping on a Pt-plate at 1200 °C for 10 h in air. The TEM samples were prepared by mechanical grinding of sintered samples to a thickness of 100 μm, dimpling to a thickness of less than 10 μm and ion-beam thinning for electron transparency. The microstructures of the samples were observed via SEM on cross-sections of the samples after polishing to a 0.25 μm finish and thermal etching at 1050 °C for 20 min in air. Grain size distributions were measured from SEM micrographs using an image analysis program (Matrox Inspector 2.1, Matrox Electronic Systems, Ltd., Dorval, Canada). At least 400 grains were measured for each sample and then the two-dimensional size distributions were presented as grain size distribution data.

3. Results and discussion

The shape of grains in a solid–liquid two-phase system with a low volume fraction of liquid can be revealed at triple junctions with liquid pockets.[8,23,25] Fig. 3 shows TEM micrographs of undoped (0T), 0.7 mol% TiO_2-doped (0.7T), and 1.5 mol% TiO_2-doped NBT–5BT (1.5T) samples sintered at 1200 °C for 1 h. As the crystal structure of NBT–5BT is pseudo-cubic (rhombohedral with $a = b = c = 3.8864$ Å and $\alpha = \beta = \gamma = 89.2°$),[28,29] the selected area diffraction patterns in the insets of the figure indicate that the crystallographic planes of the three different grains have (0 0 1) orientation.

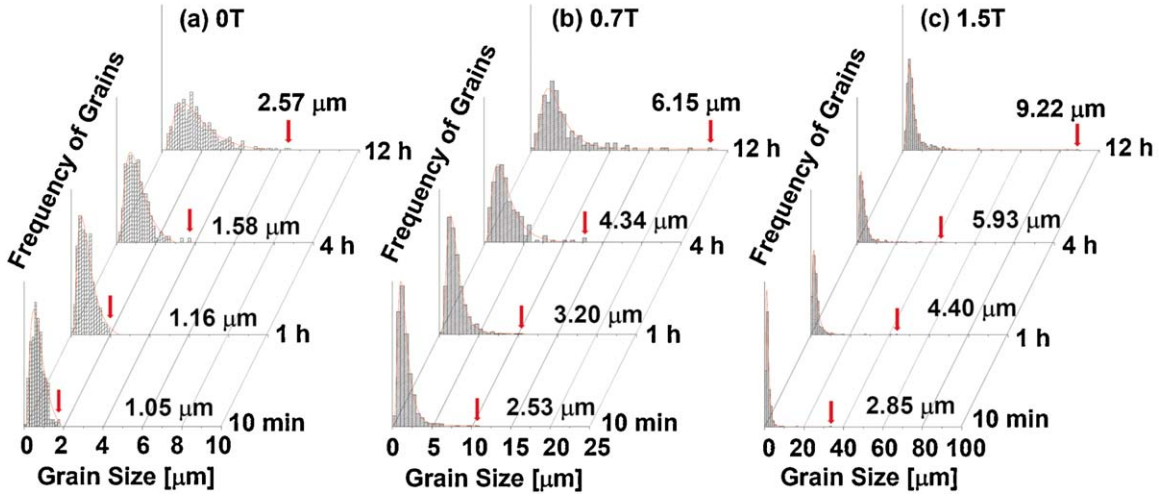

Fig. 6. Grain size distributions and average grain sizes of (a) undoped (0T), (b) 0.7 mol% (0.7T), and (c) 1.5 mol% TiO_2-doped NBT–5BT (1.5T) sintered at 1200 °C for various times. The largest grain in each sample is indicated by an arrow.

The grain shapes, however, are slightly different from each other, although they are all round-edged cubes. As the concentration of added TiO_2 is increased, the area of rounded corners decreases and the grains become more faceted, indicating that the step free energy of the (1 0 0) plane increases with increasing TiO_2 addition. A similar change in grain shape also occurred at the surface of the bulk samples, as shown in Fig. 4, where the 3-dimensional grain shape of a round-edged cube is clearly revealed. This change in grain shape is expected to affect the grain coarsening behavior, because the growth kinetics of round-edged grains is governed by the growth of facet planes.[23]

The microstructures in Fig. 5 and their grain size distributions in Fig. 6, indeed, show that the coarsening behavior changes considerably with the addition of TiO_2. In NBT–5BT samples, the size distribution broadens as the sintering time increases. Nevertheless, the size distribution is apparently unimodal for a few hours, indicating that the coarsening behavior is pseudo-normal. As the sintering time is increased, abnormal grains, with sizes several times the average size, appear, showing a change in grain coarsening behavior (Figs. 5(a) and 6(a)). This behavior was already reported in our previous investigation.[23] In the case of 0.7 mol% TiO_2-doped samples (0.7T), however, several large grains form at the beginning of sintering (10 min) and these grains grow abnormally (Figs. 5(b) and 6(b)). The AGC behavior is intensified in samples with 1.5 mol% TiO_2 addition (Figs. 5(c) and 6(c)). From the beginning, a few abnormal grains form and grow considerably as the sintering proceeds. As shown in Figs. 5 and 6, with an increasing amount of TiO_2, the size difference between the abnormal grains and the matrix grains increases; however, the number of abnormal grains decreases.

The observed grain coarsening behavior with respect to the amount of TiO_2 and the sintering time can be explained by the nonlinear migration behavior of faceted solid/liquid interfaces with different step free energies. Fig. 1 schematically plots the growth rates of a grain in samples with different amounts of TiO_2 addition as a function of the driving force. The critical driving force for appreciable growth, Δg_c, increases with increased TiO_2 addition, as the grain takes on a more faceted shape with a higher step free energy. When the maximum driving force exceeds the critical driving force in the 1.5T samples, large grains having driving forces greater than $\Delta g_c^{1.5T}$ grow rapidly and become abnormal grains, as observed in Fig. 5(c). For the 0.7T samples, however, the number of large grains with driving forces greater than $\Delta g_c^{0.7T}$ exceeds that in the 1.5T samples. The number of abnormal grains is also larger but their size is smaller than that in the 1.5T samples after impingement of abnormal grains, as observed in Fig. 5(b). In the case of 0T samples, the number of grains with the driving forces larger than Δg_c^{0T} is very high; as a result, many grains grow considerably, initially showing PNGC behavior. However, as Δg_{max} decreases towards Δg_c^{0T} with overall grain coarsening, some abnormal grains form after a certain period of time, as observed in Figs 5(a) and 6(a).[23] This type of AGC is different from the commonly observed incubated AGC in highly faceted systems, where Δg_{max} is smaller than Δg_c. In the case of the incubated AGC, the grain growth rate is very low, even for the largest grain, and it is expressed as an exponential function of the driving force for 2-dimensional nucleation and growth.[20,30,31] (Even in the presence of surface defects, the growth rate can be governed by 2-dimensional nucleation and growth with the same functional dependence.[32,33]) Nevertheless, as the largest grain has the highest (relative) growth rate, the size distribution broadens and the driving force of the largest grain can increase beyond Δg_c after a certain period of time, resulting in the belated formation of abnormal grains.[19,27] This type of incubated AGC is usually not observed in systems with moderate step free energies, as in our NBT–BT system.

The observed change in the grain shape with the addition of TiO_2 and the resultant grain coarsening behavior with respect to time experimentally confirm our previous theoretical prediction, which is based on the coupling effect of Δg_c and Δg_{max},[19,20] regarding the effect of the step free energy on the grain coarsening behavior. The recently observed incubated AGC in the $BaTiO_2$–TiO_2–SiO_2 system[27] also confirms this theoretical prediction.

4. Conclusion

With the addition of TiO_2, grain shape and grain coarsening behavior in the $95Na_{1/2}Bi_{1/2}TiO_2$–$5BaTiO_3$ system change towards more faceted and abnormal, respectively. The change in grain shape indicates an increase in step free energy, and hence a rise in the critical driving force for appreciable growth. This suggests a reduction of the number of grains that have driving forces larger than the respective critical driving force for appreciable growth, Δg_c. This explains the increased tendency of abnormal grain coarsening with TiO_2 addition. These experimental observations and explanations support the theoretical prediction based on the coupling effects between Δg_c and Δg_{max} (the maximum driving force for growth).

Acknowledgements

This research was supported by a grant from the Center for Advanced Materials Processing (CAMP) of the 21st Century Frontier R&D Program funded by the Ministry of Knowledge Economy (MKE), Republic of Korea under Grant No. PM007-10-01-01 and also by Priority Research Centers Program through the National Research Foundation of Korea (NRF) funded by the Ministry of Education, Science and Technology (2009-0094039).

References

1. Warren R. Microstructural development during liquid-phase sintering of VC–Co alloys. *J Mater Sci* 1972;**7**(12):1434–42.
2. Kang CH, Yoon DN. Coarsening of cobalt grains dispersed in liquid copper matrix. *Metall Mater Trans A* 1981;**13A**:65–9.
3. Kang SS, Yoon DN. Kinetics of grain coarsening during sintering of Co–Cu and Fe–Cu alloys with low liquid contents. *Metall Mater Trans A* 1982;**13A**:1405–11.
4. Kang SJL, Han SM. Grain-growth in Si_3N_4-based materials. *MRS Bull* 1995;**20**(2):33–7.
5. Park YJ, Hwang NM, Yoon DY. Abnormal growth of faceted (WC) grains in a (Co) liqiud matrix. *Metall Mater Trans A* 1996;**27**(9):2809–19.
6. Kwon SK, Hong SH, Kim DY, Hwang NM. Coarsening behavior of tricalcium silicate (C_3S) and dicalcium silicate (C_2S) grains dispersed in a clinker melt. *J Am Ceram Soc* 2000;**83**(5):1247–52.
7. Park CW, Yoon DY. Effects of SiO_2, CaO_2, and MgO additions on the grain growth of alumina. *J Am Ceram Soc* 2000;**83**(10):2605–9.
8. Chung SY, Yoon DY, Kang SJL. Effects of donor concentration and oxygen partial pressure on interface morphology and grain growth behavior in $SrTiO_3$. *Acta Mater* 2002;**50**(13):3361–71.
9. Jang CW, Kim J, Kang SJL. Effect of sintering atmosphere on grain shape and grain growth in liquid-phase-sintered silicon carbide. *J Am Ceram Soc* 2002;**85**(5):1281–4.
10. Choi K, Hwang NM, Kim DY. Effect of grain shape on abnormal grain growth in liquid-phase-sintered $Nb_{1-x}Ti_xC$–Co alloys. *J Am Ceram Soc* 2002;**85**(9):2313–8.
11. Kim MJ, Yoon DY. Effect of magnesium oxide addition on surface roughening of alumina grains in anorthite liquid. *J Am Ceram Soc* 2003;**86**(4):630–3.
12. King PT, Gorzkowski EP, Scotch AM, Rockosi DJ, Chan HM, Harmer MP. Kinetics of {0 0 1} $Pb(Mg_{1/3}Nb_{2/3})O_3$–35 mol% $PbTiO_3$ single crystals grown by seeded polycrystal conversion. *J Am Ceram Soc* 2003;**86**(12):2182–7.
13. Park CW, Yoon DY, Blendell JE, Handwerker CA. Singular grain boundaries in alumina and their roughening transition. *J Am Ceram Soc* 2003;**86**(4):603–11.
14. Cho YK, Yoon DY, Kim BK. Surface roughening transition and coarsening of NbC grains in liquid cobalt-rich matrix. *J Am Ceram Soc* 2004;**87**(3):443–8.
15. Yoon BK, Lee BA, Kang SJL. Growth behavior of rounded (Ti,W)C and faceted WC grains in a Co matrix during liquid phase sintering. *Acta Mater* 2005;**53**(17):4677–85.
16. Jo W, Kim DY, Hwang NM. Effect of interface structure on the microstructural evolution of ceramics. *J Am Ceram Soc* 2006;**89**(8):2369–80.
17. Kim MS, Fisher JG, Kang SJL, Lee HY. Grain growth control and solid-state crystal growth by Li_2O/PbO addition and dislocation introduction in the PMN–35PT system. *J Am Ceram Soc* 2006;**89**(4):1237–43.
18. Sano T, Rohrer GS. Experimental evidence for the development of bimodal grain size distributions by the nucleation-limited coarsening mechanism. *J Am Ceram Soc* 2007;**90**(1):211–6.
19. Jung YI, Yoon DY, Kang SJL. Coarsening of polyhedral grains in a liquid matrix. *J Mater Res* 2009;**24**(9):2949–59.
20. Kang SJL, Lee MG, An SM. Microstructural evolution during sintering with control of the interface structure. *J Am Ceram Soc* 2009;**92**(7):1464–71.
21. Lifshitz IM, Slyozov VV. The kinetics of precipitation from supersaturated solid solutions. *J Phys Chem Solids* 1961;**19**:35–50.
22. Wagner C. Theory of precipitate change by redissolution. *Z Elechem* 1961;**65**:581–91.
23. Moon KS, Kang SJL. Coarsening behavior of round-edged cubic grains in the $Na_{1/2}Bi_{1/2}TiO_3$–$BaTiO_3$ system. *J Am Ceram Soc* 2008;**91**(10):3191–6.
24. Fisher JG, Kim MS, Lee HY, Kang SJL. Effect of Li_2O and PbO additions on abnormal grain growth in the $Pb(Mg_{1/3}Nb_{2/3})O_3$–35 mol% $PbTiO_3$ system. *J Am Ceram Soc* 2004;**87**(5):937–42.
25. Fisher JG, Choi SY, Kang SJL. Abnormal grain growth in barium titanate doped with alumina. *J Am Ceram Soc* 2006;**89**(7):2206–12.
26. Fisher JG, Kang SJL. Microstructural changes in $(K_{0.5}Na_{0.5})NbO_3$ ceramics sintered in various atmospheres. *J Eur Ceram Soc* 2009;**29**(12):2581–8.
27. Heo YH, Jeon SC, Fisher JG, Choi SY, Hur KH, Kang SJL. Effect of step free energy on delayed abnormal grain growth in a liquid phase-sintered $BaTiO_3$ model system. *J Eur Ceram Soc* 2011;**31**(5):755–62.
28. Smolenskii GA, Isupov VA, Agranovska AI, Kainik NN. New ferroelectrics of complex composition. *Sov Phys Solid State* 1961;**2**(11):2651–4.
29. Ge W, Liu H, Zhao X, Pan X, He T, Lin D, et al. Growth and characterization of $Na_{0.5}Bi_{0.5}TiO_3$–$BaTiO_3$ lead-free piezoelectric crystal by the TSSG method. *J Alloy Compd* 2008;**456**(1–2):503–7.
30. Hirth JP, Pound GM. *Condensation and evaporation: nucleation and growth kinetics*. Oxford: Pergamon Press; 1963. p. 77–148.
31. Howe JM. *Interfaces in materials*. New York: John Wiley & Sons; 1997. p. 256–68.
32. Bennema P, van der Eerden JP. Crystal graphs, connected nets, roughening transition and the morphology of crystals. In: Sunagawa I, editor. *Morphology of crystals*. Tokyo, Japan: Terra Scientific Publishing Company; 1987. p. 1–75.
33. Kang MK, Yoo YS, Kim DY, Hwang NM. Growth of $BaTiO_3$ seed grains by the twin-plane reentrant edge mechanism. *J Am Ceram Soc* 2000;**83**:385–90.